

The Gene for Human Fibronectin Glomerulopathy Maps to 1q32, in the Region of the Regulation of Complement Activation Gene Cluster

Martin Vollmer,¹ Martin Jung,² Franz Rüschemdorf,² Rainer Ruf,¹ Thomas Wienker,³ André Reis,² Reto Krapf,⁴ and Friedhelm Hildebrandt¹

¹University Children's Hospital, Freiburg University, Freiburg, Germany; ²Mikrosatellitenzentrum, Max-Delbrück-Centrum, Berlin; ³Institut für Medizinische Statistik, Dokumentation und Datenverarbeitung, Universität Bonn, Bonn; and ⁴Department of Internal Medicine, Bruderholzspital, Bruderholz, Switzerland

Summary

Fibronectin glomerulopathy (GFND) is a newly recognized autosomal dominant disease of the kidney that results in albuminuria, microscopic hematuria, hypertension, renal tubular acidosis type IV, and end-stage renal disease in the 2d to 6th decade of life. The disease is characterized histologically by massive deposits of fibronectin (Fn) present in the subendothelial spaces of renal glomerular capillaries. The cause of human GFND is unknown. In order to localize a candidate gene for GFND, we performed linkage analysis of a large, 193-member pedigree containing 13 affected individuals. Since we had previously excluded the genes for Fn and uteroglobin as candidate genes for GFND, a total-genome search for linkage was performed. Examination of 306 microsatellite markers resulted in a maximum two-point LOD score of 4.17 at a recombination fraction of .00 for marker D1S249, and a maximum multipoint LOD score of 4.41 for neighboring marker D1S2782. By detection of recombination events, a critical genetic interval of 4.1 cM was identified, which was flanked by markers D1S2872 and D1S2891. These findings confirm that GFND is a distinct disease entity among the fibrillary glomerulopathies. Gene identification will provide insights into the molecular interactions of Fn in GFND, as well as in genetically unaltered conditions.

Introduction

Glomerular fibrillary deposits have been described in three different disease entities: amyloidosis, immunotactoid glomerulonephritis, and fibrillary glomerulopathy (Alpers et al. 1987; Korbet et al. 1991, 1994; Alpers 1992, 1993; Fogo et al. 1993; Hildebrandt and Vollmer 1998). Fibronectin glomerulopathy (GFND; MIM 601894) is a newly recognized autosomal dominant kidney disease, which has been distinguished from these other disease entities by the presence of glomerular fibrillary deposits that show strong immune reactivity to fibronectin (Fn; Strøm et al. 1995). Patients with GFND develop albuminuria, microscopic hematuria, arterial hypertension, renal tubular acidosis type IV, and end-stage renal disease (ESRD) in the 2d to 6th decade of life, which necessitates renal replacement therapy by dialysis or renal transplantation (Strøm et al. 1995). Although individual unrelated families with GFND have been reported elsewhere (Bürgin et al. 1980; Tuttle et al. 1987; Abt et al. 1991; Mazzucco et al. 1992; Assmann et al. 1995), the condition was recognized as a new disease entity by Strøm et al. (1995), after the histologic findings were reexamined in all six reported families. The genetic defect in GFND is unknown.

Renal histology examination reveals glomeruli that are enlarged, with minimal hypercellularity and with the presence of giant fibrillary deposits in the renal glomerular capillaries (Bürgin et al. 1980). Electron microscopy examination reveals that the deposits are mainly located in the subendothelial space but are also in the subepithelial and intramembranous spaces. There is only scant immunoreactivity for immunoglobulins or for complement factors C1, C3, and C4. However, deposits are strongly immunoreactive for antibodies to Fn (Strøm et al. 1995). Fn is an adhesive, high-molecular weight glycoprotein that is found in extracellular matrices, such as the glomerular basement membrane. Fn takes part in cellular proliferation, wound healing, and platelet aggregation. Because Fn stimulates endocytosis and promotes the clearance of particulate material from the circulation, it has been suggested to function in the

Received July 30, 1998; accepted for publication October 14, 1998; electronically published November 25, 1998.

Address for correspondence and reprints: Dr. Friedhelm Hildebrandt, University Children's Hospital, Freiburg University, Mathildenstrasse 1, D-79106 Freiburg, Germany. E-mail: hildebra@sun1.ukl.uni-freiburg.de

© 1998 by The American Society of Human Genetics. All rights reserved.
0002-9297/98/6306-0019\$02.00

clearance of C1q-coated material, such as immune complexes or cellular debris (Bing et al. 1982).

In the large GFND kindred examined in this study, samples studied by use of electron microscopy were clearly fibrillary and consisted of nonoriented 12×125 -nm fibers (Bürgin et al. 1980). In immunolocalization studies, the fibrillary deposits stained positively with use of an antibody detecting both plasma-derived Fn and cellular Fn but were only weakly positive with use of an antibody detecting only cellular Fn. The fibrils, therefore, were identified as deposits of plasma-derived Fn (Strøm et al. 1995). In one patient, the Fn deposits recurred in a transplanted kidney, although there was no indication of systemic deposition of Fn (Gemperle et al. 1996). These findings strongly suggested a molecular defect in the binding behavior of circulating Fn that influenced its glomerular handling, which led to renal glomerular deposition of Fn.

In a recent study by Zhang et al. (1997), a mouse model of targeted gene disruption of the *uteroglobin* (*UG*) gene was described. In this animal model, mice developed severe renal disease in association with massive glomerular deposits of Fn. The distribution of these deposits and the clinical course were highly reminiscent of human GFND. The molecular mechanism by which *UG* normally prevents Fn deposition in the glomerulus appears to involve high-affinity binding of *UG* to Fn, in

circulating blood, to form Fn-UG heteromers. These Fn-UG heteromeric complexes were shown to counteract Fn self-aggregation, which resulted in abnormal renal glomerular Fn deposition in this knockout-mouse model. The striking similarity between the Fn-UG knockout-mouse model and human GFND raised the possibility that an analogous pathogenic mechanism may underlie GFND. In a previous study of a mouse model of targeted disruption of the *UG* gene, the same phenotype had not been observed (Stripp et al. 1996). We previously had examined the hypothesis that a genetic defect in the genes for Fn or *UG* was responsible for GFND. By use of haplotype analysis of the large GFND pedigree reported here, we excluded the genes for Fn, villin, and desmin, as well as the *UG* gene, from being the causative genes for GFND (Hildebrandt et al. 1996; Vollmer et al. 1998).

In the present study, therefore, we conducted a total-genome search for linkage, which resulted in the localization of a gene locus for GFND to a 4.1-cM genetic interval, between markers D1S2872 and D1S2891, on chromosome 1q32, with a maximum multipoint LOD score (Z_{\max}) of 4.41 for marker D1S2782. These findings confirm GFND as a distinct disease entity. Gene identification will provide insights into the molecular interactions of Fn in GFND, as well as insights into the normal function of Fn.

Patients and Methods

Patients

Selected patients from the 193-member, five-generation GFND pedigree examined in this study were initially described by Bürgin et al. (1980). We collected blood samples from 99 individuals from this pedigree, for isolation of genomic DNA, after we obtained informed consent. The clinical course of 157 individuals of this kindred, 13 of whom were affected by GFND, was described in a 15-year follow-up study by Gemperle et al. (1996). Histological aspects of these subjects have been described elsewhere (family F in Strøm et al. 1995). Segregation of GFND in this pedigree is consistent with autosomal dominant inheritance and exhibits age-related penetrance.

Thirteen relatives had developed ESRD based on GFND. The definition of affected status, as described by Bürgin et al. (1980), was made on the basis of a biopsy sample compatible with GFND from nine of the affected individuals. For the other four individuals (201, 411, 305, and 311), the clinical history was clearly compatible with an affected status. For the definition of absence of GFND symptoms, the following criteria had to be met: (1) absence of significant proteinuria; (2) normal blood pressure (<140/90 mm Hg), adjusted for age in children;

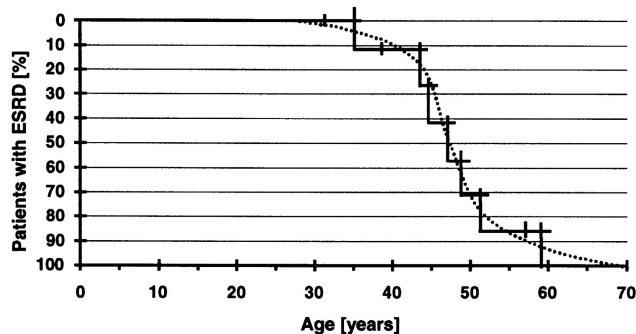


Figure 1 Kaplan Meier analysis of renal death in 10 patients from the large GFND kindred. In 10 of 13 affected individuals, data on onset of ESRD were available. Start of renal replacement therapy or death as a result of uremia was defined as “renal death.” Three patients were censored, since renal death did not occur during the observation period. (Censoring is indicated by vertical strokes without a drop in the survival curve.) Patient 544, who is affected by GFND, was censored at age 32 years, for normal creatinine clearance of 98 ml/min; patient 465 was censored at age 37 years, when death occurred as a result of a nonrenal cause; and patient 462, who is affected by GFND, was censored at age 58 years, when creatinine clearance was reduced only to 57 ml/min. The median “renal survival time” was 47 years (range 34–59 years). A curve was fitted manually (dotted line) for estimation of liability classes (see Patients and Methods). Entries (vertical strokes) represent patients in the following order: individuals 544, 311, 465, 461, 452, 468, 451, 454, 462, and 463 (see fig. 4).

(3) normal renal function (plasma creatinine concentration <1.0 mg/dl and creatinine clearance >120 ml/min), adjusted for age in children; and (4) normal urine sediment (Gemperle et al. 1996). In one patient (452; see fig. 4), the disease recurred in the renal allograft after transplantation, and another patient (463) developed organ-limited renal cell carcinoma, as did his unaffected younger sister (467; Gemperle et al. 1996). In three additional patients, the disease had not yet recurred 13, 4, and 2 years after renal transplantation.

Linkage Analysis

Linkage analysis was performed by use of 297 microsatellite markers from the Max-Delbrück Center-microsatellite set, with an average spacing of 11 cM (M. Jung, personal communication), and by use of 9 additional microsatellites, for further fine mapping (Dib et al. 1996). Genomic DNA was isolated, by use of standard methods (Sambrook et al. 1989), directly from blood samples or was isolated after Epstein-Barr virus

(EBV) transformation of peripheral blood lymphocytes (Steel et al. 1977). Microsatellite markers were amplified individually by use of an MJ Research Multicycler PTC225 Tetrad (Biozym). After pooling, markers were separated by use of an ABI377XL DNA sequencer using GENESCAN software, as described elsewhere (Hildebrandt et al. 1993b; Saar et al. 1997).

For GFND an autosomal dominant mode of inheritance with age-related penetrance was assumed on the basis of clinical and pedigree data (Strom et al. 1995). Two-point LOD scores between the disease locus and microsatellite markers were calculated by use of the MLINK subroutine of the computer program package LINKAGE 5.01 (Lathrop et al. 1984). The gene frequency of GFND was set at .0001. The ILINK component of the LINKAGE package was used to calculate Z_{\max} and maximum recombination fractions (θ_{\max}). Non-parametric linkage analysis was performed by use of GENEHUNTER (Kruglyak et al. 1996). To conduct multipoint linkage analysis, the program VITESSE was used (O'Connell and Weeks 1995). Intermarker distances were taken from Dib et al. (1996), and further ordering of microsatellite markers was performed by use of sequence tagged-site (STS) content mapping of CEPH YAC clones (data not shown). Haplotype analysis was evaluated graphically (see fig. 4) by use of CYRILLIC, version 2.1.3 (Cherwell Scientific).

In accordance with the data on age-related penetrance in this pedigree (fig. 1), liability classes were assigned as follows: Affected subjects with GFND and unaffected subjects of the second generation were assigned liability class 1, with the penetrance vector $\{.0, .0, .0\}$. Unaffected individuals in the third or fourth generation were assigned liability class 2, with penetrance vector $\{.0, .95, 1.0\}$, if the individual was >50 years of age. Liability class 3, with penetrance vector $\{.0, .70, .0\}$, was assigned if the individual was <50 years of age.

Results

A subset of the large GFND pedigree, of 13 affected individuals and 55 individuals without symptoms of GFND, was employed in the linkage analysis using a total-genome search. Fifteen years after the initial description made by Bürgin (1980), individuals of the large GFND pedigree had been reexamined for the presence or absence of GFND symptoms (Gemperle et al. 1996), in accordance with the criteria described in Patients and Methods. For the present study, 20 individuals of the youngest generation (all ≤ 39 years of age), who showed no symptoms of GFND in the previous study, were reexamined for affection status, by use of the same criteria. At reexamination, there was low-grade proteinuria in three individuals (481, 571, and 551). In one patient (481), there was arterial hypertension, and in two pa-

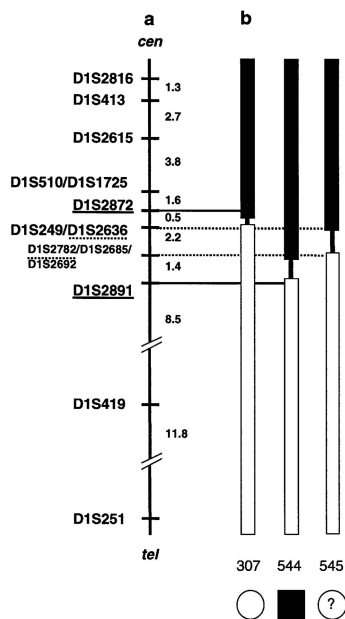


Figure 2 *a*, Genetic map of the GFND region on chromosome 1q32. Microsatellite markers are left of the map axis, and sex-averaged genetic distances (centimorgans) are to the right. Flanking markers are underlined. cen = centromere, and tel = telomere. *b*, Recombinant events, identified by haplotype analysis (see fig. 4). The haplotype associated with GFND disease status is represented by a blackened bar; the haplotype associated with the unaffected status is represented by an unblackened bar. Individual numbers and symbols for sex and affected status are shown below the bars (see fig. 4). Flanking markers D1S2872 and D1S2891 are defined by recombinant events in individuals 307 and 544, respectively. Markers are underlined and connected to haplotype bars by solid or dotted lines to indicate certain or potential flanking markers, respectively.

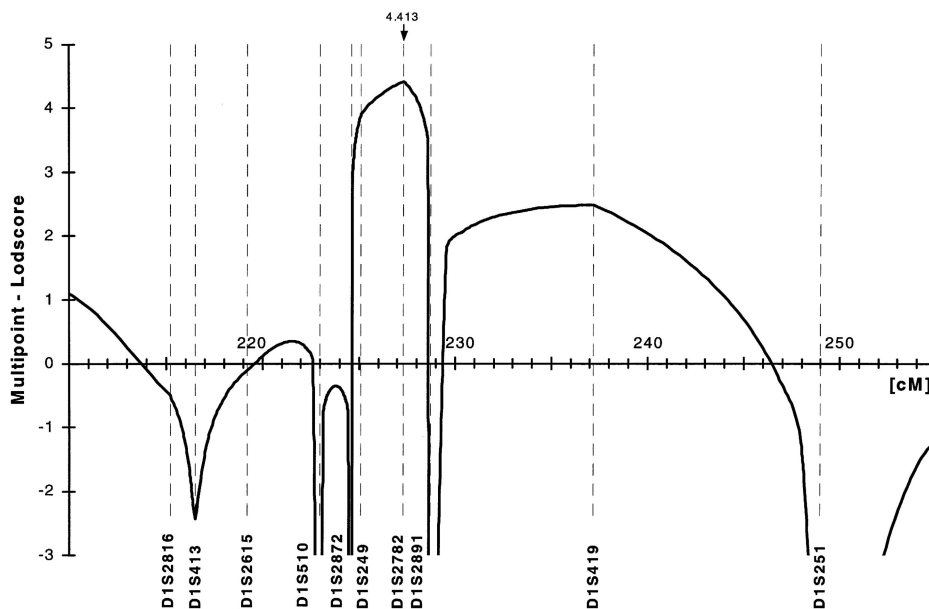


Figure 3 Multipoint linkage analysis of the large GFND pedigree. Six marker loci were calculated versus a *GFND* locus, by use of VITESSE. Vertical dashed lines indicate positions of microsatellite markers (see fig. 2a). Intermarker distances were taken from the report by Dib et al. (1996) and from STS content mapping of CEPH YAC clones (data not shown). For marker D1S2782, $Z_{\max} = 4.413$, as indicated.

tients (592 and 545), there was insufficient data for classification. Because low-grade proteinuria is known not to cosegregate with the disease status (Gemperle et al. 1996), these data are not sufficient for diagnosis of GFND. Therefore, no additional information regarding affected status can be derived from these data.

Age-Related Penetrance

Because of age dependency for the development of ESRD in GFND, the absence of ESRD cannot be determined with certainty before age 60 years. We therefore related disease penetrance to age in this large GFND pedigree. Kaplan Meier survival analysis of "renal death" was performed for 10 of the 13 affected individuals of the large GFND pedigree, for whom data for onset of ESRD was available (fig. 1). Start of renal replacement therapy or death as a result of uremia was defined as "renal death." Three patients were censored, since renal death did not occur during the observation period. The median "renal survival time" was 47 years (range 34–59 years). A curve was fitted to the survival function, which showed a homogeneous, symmetric, sigmoidal shape for the time course of development of ESRD in this family.

Total-Genome Search

A total-genome search using 297 microsatellite markers from the MDC-marker set (M. Jung, personal communication) was performed, as described elsewhere

(Saar et al. 1997), in a subset of the large GFND pedigree, which contained 13 affected individuals and 55 individuals without symptoms for GFND. The highest two-point LOD score, as detected by LODVIEW as a screening procedure (Hildebrandt et al. 1993a), was 1.65 ($\theta = .05$) at marker D1S419. For fine mapping of this candidate region, nine additional microsatellite markers in this region (Dib et al. 1996) were genotyped. Intermarker distances were taken from the report by Dib et al. (1996). These markers span an interval of 33.8 cM, a sex-averaged genetic distance, on chromosome 1q32, in the following order: cen–D1S2816–1.3 cM–D1S413–2.7 cM–D1S2615–3.8 cM–D1S510–1.6 cM–D1S2872–0.5 cM–D1S249–2.2 cM–D1S2782–1.4 cM–D1S2891–8.5 cM–D1S419–11.8 cM–D1S251–tel (fig. 2a).

Since there was age dependency for the development of ESRD, liability classes were assigned according to age at examination, as described in Patients and Methods. In addition, an "affected-only" strategy was used, which is most robust against age-related penetrance, at the expense of informativity. Two-point linkage analysis resulted in $Z_{\max} = 4.17$ ($\theta = .00$) for marker D1S249 (table 1). We thus generated significant evidence for linkage of a *GFND* locus to this genetic region on human chromosome 1q. When the affected-only strategy was used, a $Z_{\max} = 2.1$ ($\theta = .00$) for marker D1S249 was obtained. Haplotype analysis with six microsatellite markers, by use of VITESSE, yielded $Z_{\max} = 4.41$ for marker

Table 1
Pairwise LOD Scores Reflecting Linkage Between Chromosome 1q Loci and GFND

LOCUS	LOD SCORE AT θ						Z_{\max} (AT θ_{\max})
	.00	.01	.05	.1	.2	.3	
D1S2816	.181	.199	.251	.282	.275	.211	.282 (.1)
D1S413	.432	.455	.533	.597	.620	.518	.620 (.2)
D1S2615	1.338	1.325	1.271	1.189	.966	.656	1.338 (.0)
D1S510	-1.053	-.757	-.256	.011	.220	.243	.243 (.3)
D1S2872	$-\infty$	-1.168	-.347	.013	.262	.243	.262 (.2)
D1S249	4.173	4.117	3.877	3.544	2.771	1.849	4.173 (.0)
D1S2636	.764	.757	.722	.663	.511	.317	.764 (.0)
D1S2782	2.365	2.368	2.363	2.286	1.926	1.356	2.368 (.01)
D1S2796	1.577	1.552	1.449	1.307	.990	.646	1.577 (.0)
D1S2685	2.273	2.246	2.126	1.956	1.547	1.046	2.273 (.0)
D1S2692	2.948	2.928	2.823	2.638	2.113	1.418	2.948 (.0)
D1S2891	$-\infty$	2.074	2.531	2.505	2.068	1.390	2.531 (.05)
D1S419	2.719	2.679	2.510	2.276	1.730	1.088	2.719 (.0)
D1S251	-7.353	-4.698	-2.625	-1.693	-.782	-.325	-.325 (.3)

NOTE.—LOD scores were calculated at various θ s, by use of liability classes, as described in Patients and Methods.

D1S2782, which is adjacent to marker D1S249 (fig. 3). Nonparametric linkage analysis using GENEHUNTER yielded $Z_{\max} = 8.0$ for marker D1S249 (data not shown).

Definition of Flanking Markers

When haplotype analyses were evaluated (fig. 4), a proximal recombination event was detected for marker D1S2872 in individual 307, who is unaffected by GFND at age 86 years, and a distal recombination event was detected for marker D1S2891 in affected individual 544 (fig. 2b). Therefore, these two markers define a critical interval for GFND of 4.1 cM of sex-averaged genetic distance. In addition, closer definition of flanking markers would be possible if the affected status for individual 545 was known. However, in the absence of symptoms for GFND at age 33 years, the affected status of this individual cannot be determined with certainty. If this subject was affected, marker D1S2782 would be identified as a closer distal-flanking marker. If this individual was unaffected, marker D1S2636 would be identified as a closer proximal-flanking marker.

Marker D1S2782, which exhibited the highest Z_{\max} , is positioned on CEPH YAC clones 908_e_12 (1,230 kb) and 928_b_8 (1,190 kb) (Whitehead/MIT Center for Genome Research). In addition to this marker, we localized, by use of STS content mapping, several expressed sequence tags (ESTs) for genes of the regulation of complement activation (RCA) gene cluster to these two YAC clones (data not shown). Among these were EST WI-17154, for the decay-accelerating factor for complement (DAF) gene; EST SGC35372, for the complement component (3b/4b) receptor-1 (CR1) gene; and

EST M26021, for the complement component (3d/EBV) receptor-2 (CR2) gene. All three genes had been localized previously to 1q32 (Weis et al. 1984; Lemons et al. 1987). ESTs and polymorphic markers were positioned, by use of STS content mapping, in the region of overlap between both YAC clones (908_e_12 and 928_b_8), in the following order: cen-M26021-WI-17154-DAF-CR2-D1S2782-D1S2796-SGC35372-CR1-SHGC12033-MCP-D1S2891-tel.

The gene for factor H, another regulator of complement activation, was localized outside of the critical interval, by STS content mapping (data not shown). From the data presented, we concluded that a gene locus for GFND in this family is localized within a 4.1-cM interval on chromosome 1q32, between markers D1S2872 and D1S2891, in close vicinity to the RCA gene cluster. These findings confirm GFND as a distinct disease entity among the fibrillary glomerulopathies.

Discussion

In a large GFND pedigree that has been extensively characterized clinically, we performed linkage analysis by using a total-genome search strategy, which resulted in chromosomal localization of a gene locus for GFND to chromosome 1q32, with $Z_{\max} = 4.41$ for marker D1S2782. The 4.1-cM critical genetic interval for GFND was flanked by markers D1S2872 and D1S2891, and contained the RCA gene cluster.

The age at onset of early symptoms, as well as the age at onset of terminal renal failure, seems to vary among the different GFND pedigrees described in the literature and seems to be relatively consistent within the

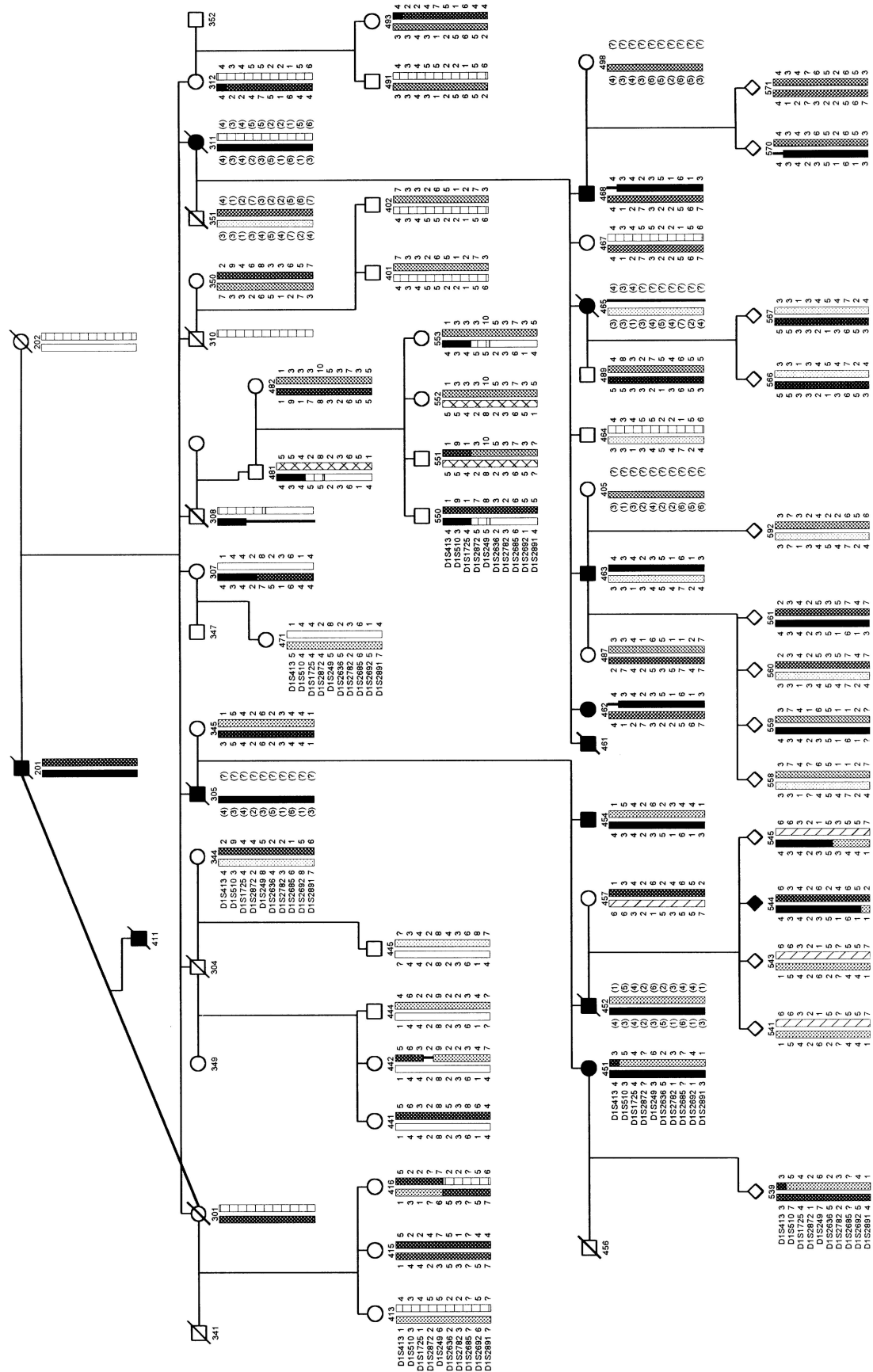


Figure 4 Haplotype analysis of 10 consecutive microsatellite markers (also see fig. 2a) of the *GFND* locus on 1q32 in 13 affected and 55 unaffected individuals of the large GFND pedigree. Sibs are ordered, from left to right, by descending age. Below the symbols, individuals are numbered. Microsatellite loci are given in the first column. Haplotypes that are associated with the affected status are depicted by a blackened bar. Recombinant events were detected for marker D1S2872 in individual 307 and for marker D1S2891 in individual 544 (also see legend to fig. 2).

same family. In the families reported by Abt (1991), Tuttle (1987), and Mazzucco (1992), terminal renal failure developed at ages 20–40 years, whereas in the large pedigree studied here, terminal renal failure clearly showed a later age at onset, between 34–59 years.

Pathogenetic Hypothesis

In GFND, several histologic and clinical characteristics indicate a genetic defect leading to altered binding behavior of circulating Fn. (1) Strong immunostaining with antibodies against plasma-derived Fn was a consistent finding in the GFND families described (Strøm et al. 1995). (2) The recurrence of disease in one transplanted kidney in individual 452 indicates that the genetic defect manifests itself independently of expression of the defective gene product in the kidney. This points to a genetic defect in a circulating factor, which might interfere with the glomerular handling of the deposited material. (3) *UG* knockout mice developed severe renal disease with massive glomerular deposits of Fn, with a clinical time course and deposit distribution highly reminiscent of human GFND (Zhang et al. 1997). Although there is no *UG* expression in the kidney, Zhang and colleagues demonstrated that *UG* normally prevents Fn deposition in the glomerulus through high-affinity binding of *UG* to Fn in circulating blood, to form Fn-*UG* heteromers. These Fn-*UG* heteromeric complexes were shown to counteract Fn self-aggregation, which resulted in abnormal renal Fn deposition. Because the *UG* gene has been excluded as causative for GFND in this pedigree (Vollmer et al. 1998), we postulate that the genetic defect lies in the gene for another protein that leads to the intramembranous trapping of Fn in the glomerular basement membrane, through altered Fn-binding properties, and, as a result, to the clinical sequelae of GFND.

Candidate Genes

The critical genetic region defined by this study contains the RCA gene cluster, which under this hypothesis contains several candidate genes for GFND, such as the *DAF*, *CR1*, and *CR2* genes. Several lines of evidence point toward a gene from the RCA cluster as a candidate gene for GFND. (1) Renal histology in GFND is very similar to that in other forms of membranoproliferative (mesangiocapillary) glomerulonephritis (MPGN), with predominance of subendothelial deposits (Bürgin et al. 1980; Gemperle et al. 1996). (2) MPGN type II is associated in ~70% of cases, with constant hypocomplementemia of factors C3, C5, and properdin, through alternate pathway activation by C3 nephritic factor. At the microscopic level, there are dense deposits of unknown origin, which stain mainly for the presence of C3 in the glomerular basement membrane, as well as in

the subendothelial and subepithelial spaces. In contrast, in MPGN types I and III, there is stimulation of the classic pathway, with low serum C1q, C2, and C4, along with C3. In MPGN, low serum C3 levels have been implicated in retardation of the normal clearing of immune complexes from the circulation (McEnery and Strife 1984; Barbiano di Belgiojoso and Ferrario 1997). (3) Compound heterozygote loss-of-function mutations of factor H, another regulator of complement activation, have been described in a patient with MPGN type II (Ault et al. 1997). However, we localized the gene for factor H outside the critical GFND region.

These findings strongly suggest a role of a gene from the RCA cluster as a candidate gene for GFND. Gene identification in GFND will provide insights into the molecular interactions of Fn in the diseased state of GFND, as well as under genetically unaltered conditions.

Acknowledgments

We thank all members of the GFND families, their physicians, and A. Koepfel, for their contributions. The excellent technical assistance of Andrea Krause and Marion Krause is gratefully acknowledged. F.H. was supported by a grant from the German Research Foundation (DFG Hi 381/3-3). F.H. and M.V. were supported by the Zentrum Klinische Forschung I (ZKF-A1) of Freiburg University (State of Baden-Württemberg). The Microsatellite Center is supported by a grant in aid of the German Genome Project (to A.R.)

Electronic-Database Information

Accession numbers and URLs for data in this article are as follows:

Online Mendelian Inheritance in Man (OMIM), <http://www.ncbi.nlm.nih.gov/Omim/> (for GFND [MIM 601894])
Whitehead/MIT Center for Genome Research Human Genetic Mapping Project data release 7, http://carbon.wi.mit.edu:8000/cgi-bin/contig/phys_map (for information on YAC clones)

References

- Abt AB, Wassner SJ, Moran JJ (1991) Familial lobular glomerulopathy. *Hum Pathol* 22:825–829
- Alpers CE (1992) Immunotactoid (microtubular) glomerulopathy: an entity distinct from fibrillary glomerulonephritis? *Am J Kidney Dis* 19:185–191
- (1993) Fibrillary glomerulonephritis and immunotactoid glomerulopathy: two entities, not one. *Am J Kidney Dis* 22:448–451
- Alpers CE, Rennke HG, Hopper J, Biava CG (1987) Fibrillary glomerulonephritis: an entity with unusual immunofluorescence features. *Kidney Int* 31:781–789

- Assmann KJM, Koene RAP, Wetzels JFM (1995) Familial glomerulonephritis characterized by massive deposits of fibronectin. *Am J Kidney Dis* 25:781–791
- Ault BH, Schmidt BZ, Fowler NL, Kashtan CE, Ahmed AE, Vogt BA, Colten HR (1997) Human factor H deficiency: mutations in framework cysteine residues and block in H protein secretion and intracellular catabolism. *J Biol Chem* 272:25168–25175
- Barbiano di Belgiojoso G, Ferrario F (1997) Membranoproliferative glomerulonephritis. In: Schrier WB, Gottschalk C (eds) *Diseases of the kidney*. Little, Brown, Boston, pp 499–520
- Bing DH, Almeda S, Isliker H, Lahav J, Hynes RO (1982) Fibronectin binds to the C1q component of complement. *Proc Natl Acad Sci USA* 79:4198–4201
- Bürgin M, Hofmann E, Reutter FW, Gürtler BA, Matter L, Briner J, Gloor F (1980) Familial glomerulopathy with giant fibrillar deposits. *Virchows Archiv* 388:313–326
- Dib C, Faure S, Fizames C, Samson D, Drouot N, Vignal A, Millasseau P, et al (1996) A comprehensive map of the human genome based on 5,264 microsatellites. *Nature* 380:152–154
- Fogo A, Qureshi N, Horn RG (1993) Morphologic and clinical features of fibrillary glomerulonephritis versus immunotactoid glomerulopathy. *Am J Kidney Dis* 22:367–377
- Gemperle O, Neuweiler J, Reutter FW, Hildebrandt F, Krapf R (1996) Familial glomerulopathy with giant fibrillar (fibronectin-positive) deposits: 15 year follow-up in a large kindred. *Am J Kidney Dis* 28:668–675
- Hildebrandt F, Pohlmann A, Omran H (1993a) LODVIEW: a computer program for the graphical evaluation of LOD-score results in exclusion mapping of human disease genes. *Comput Biomed Res* 26:502–599
- Hildebrandt F, Singh-Sawhney I, Schnieders B, Centofante L, Omran H, Pohlmann A, Schmaltz C, et al (1993b) Mapping of a gene for familial juvenile nephronophthisis: refining the map and defining flanking markers on chromosome 2. *Am J Hum Genet* 53:1256–1261
- Hildebrandt F, Strahm B, Prochoroff A, Cybulla M, Gemperle O, Krapf R, Brandis M (1996) Glomerulopathy associated with predominant fibronectin deposits: exclusion of the genes for fibronectin, villin and desmin as causative genes. *Am J Med Genet* 63:323–327
- Hildebrandt F, Vollmer M (1998) Glomerulopathies fibrillaires familiales: quel est le rôle de la fibronectine? In: Grünfeld J-P, Bach J-F, Kreis H (eds) *Actualités néphrologiques Jean Hamburger*. Médecine-Sciences Flammarion, Paris, pp 341–347
- Korbet SM, Schwartz MM, Lewis EJ (1991) Immunotactoid glomerulopathy. *Am J Kidney Dis* 17:247–257
- (1994) Current concepts in renal pathology: the fibrillary glomerulopathies. *Am J Kidney Dis* 23:751–765
- Kruglyak L, Daly MJ, Reeve-Daly MP, Lander ES (1996) Parametric and nonparametric linkage analysis: a unified multipoint approach. *Am J Hum Genet* 58:1347–1363
- Lathrop GM, Lalouel JM, Julier C, Ott J (1984) Strategies for multilocus linkage analysis in humans. *Proc Natl Acad Sci USA* 81:3443–3446
- Lublin DM, Lemons RS, Le Beau MM, Holers VM, Tykocinski ML, Medof ME, Atkinson JP (1987) The gene encoding decay-accelerating factor (DAF) is located in the complement regulatory locus on the long arm of chromosome 1. *Exp Med* 165:1731–1736
- Mazzucco G, Moran E, Rollino C, Monga G (1992) Glomerulonephritis with organized deposits: a mesangiopathic, not immune complex-mediated disease? *Hum Pathol* 23:63–68
- McEnery P, Strife CF (1984) Chronic glomerulonephritis in children. In: Tune B, Mendoza S (eds) *Pediatric nephrology*. Churchill Livingstone, New York, pp 231–246
- O'Connell JR, Weeks DE (1995) The VITESSE algorithm for rapid exact multilocus linkage analysis via genotype set-recoding and fuzzy inheritance. *Nat Genet* 11:402–408
- Saar K, Chrzanoswska KH, Stumm M, Jung M, Nurnberg G, Wienker TF, Seemanová E, et al (1997) The gene for the ataxia-telangiectasia variant, Nijmegen breakage syndrome, maps to a 1-cM interval on chromosome 8q21. *Am J Hum Genet* 60:605–610
- Sambrook J, Fritsch EF, Maniatis T (1989) *Molecular cloning: a laboratory manual*, 2d ed. Cold Spring Harbor Laboratory Press, Cold Spring Harbor, NY
- Steel CM, Philipson J, Arthur E, Gardiner SE, Newton MS, McIntosh RV (1977) Possibility of EB virus preferentially transforming a subpopulation of human B lymphocytes. *Nature* 270:729–731
- Stripp BR, Lund J, Mango GW, Kurt CD, Johnston C, Hultenby K, Nord M, et al (1996) Clara cell secretory protein: a determinant of PCB bioaccumulation in mammals. *Am J Physiol* 271:L656–L664
- Strøm EH, Banfi G, Krapf R, Abt AB, Mazzucco G, Monga G, Gloor F, et al (1995) Glomerulopathy associated with predominant fibronectin deposits: a newly recognized hereditary disease. *Kidney Int* 48:163–170
- Tuttle SE, Sharma HM, Bay W, Hebert L (1987) A unique familial lobular glomerulopathy. *Arch Pathol Lab Med* 111:726–731
- Vollmer M, Krapf R, Hildebrandt F (1998) Exclusion of the uteroglobin gene as a candidate for fibronectin glomerulopathy (GFND). *Nephrol Dial Transplant* 13:2417–2418
- Weis JJ, Tedder TF, Fearon DT (1984) Identification of a 145,000 M(r) membrane protein as the C3d receptor (CR2) of human B lymphocytes. *Proc Natl Acad Sci USA* 81:881–885
- Zhang Z, Kundu GC, Yuan CJ, Ward JM, Lee EJ, DeMayo F, Westphal H, et al (1997) Severe fibronectin-deposit renal glomerular disease in mice lacking uteroglobin. *Science* 276:1408–1412